CHARACTERIZATION OF DAMPING IN BOLTED LAP JOINTS

Christopher W. Moloney[1], Daniel M. Peairs[1], Enrique R. Roldan[2]

[1]Department of Mechanical Engineering, Virginia Polytechnic Institute and State University, Blacksburg, Va. 24061

[2]Department of Civil Engineering, The University of Texas at El Paso, El Paso, TX, 79968

ABSTRACT

The dynamic response of a jointed beam was measured in laboratory experiments. The data were analyzed and the system was mathematically modeled to establish plausible representations of joint damping behavior. Damping is examined in an approximate, local linear framework using log decrement and half power bandwidth approaches. In addition, damping is modeled in a nonlinear framework using a hybrid surface irregularities model that employs a bristles-construct. Experimental and analytical results are presented.

NOMENCLATURE

[*c*]	Viscous damping matrix
[*k*]	Stiffness matrix
[*m*]	mass matrix
[*Nk*]	Number of bristles times stiffness
[*q*]	Forcing function vector
{*R* (*x*, *x*̄) }	Vector on nonlinear restoring force
{*x*}	Displacement
?	Average fraction of bristles in contact
?, *?*$_0$, *?*$_1$	Bristle model parameters

1. INTRODUCTION

The effects of sliding friction in bolted lap joints are of great importance to the structural design community. Friction may be desirable in a mechanical design, because it dissipates energy, thereby diminishing response levels, or it may be undesirable because it dissipates energy where that effect is unwanted or makes structural control more difficult. In order to increase the utility of joint fiction in the design process, it is imperative that we establish predictive models of joint fiction behavior. Most structural dynamic analyses performed today require experiments to calibrate the damping in models, or they simply select damping based on speculation.

Friction occurs in all mechanical systems that execute structural dynamic response. Damping effects occur as the result of (1) energy dissipation at the microscopic level in materials, (2) radiation of energy into the medium that surrounds a structure (air, water, soil, or other mechanical components), (3) the interactions between elements in a structure, and (4) components that that are designed to remove energy from a system in a controlled manner.

Numerous models that characterize the behavior of frictional joints are described in the literature. These range from simple models that are used for computational convenience or to describe phenomenology in a simple manner, to more complex non-phenomenological models that match energy dissipation characteristics seen in experimental settings, to phenomenological models that seek to mimic supposed behavior at joint interfaces.

The simplest model for damping is the viscous damping model described in practically all texts on structural vibrations. (see , fore example, Inman, 1996). The simplest phenomenological model for friction is the Coulomb model described for example in Haug (1992).

Non-phenomenological models for friction seek to model damping behavior based on experimental laboratory of field observation. Examples are Stribeck's model (1902). Masing-Element models (Ottl, 1981) and the Valanis model (1971).

Phenomenological models seek to simulate damping behavior by mathematically characterizing physical

behavior of a joint. Examples are the elasto-slip model (Gaul and Nitsche) and the bristle model (Haessing and Friedland, 1991). A form of the latter will be considered in this investigation.

Gaul and Nitsche present a thorough and wide-ranging summary of friction models.

This paper presents an investigation into friction damping and vibrations of beams with bolted lap joints. Two geometrically identical specimens with different characteristics are considered. The specimens are shown schematically in Figure 1. The first specimen is a built-up beam. It consists of two long beam segments joined at the center by symmetric plates. The plates connect to the beams in a lap joint configuration, fastened with a bolt. The second specimen has geometry identical to the first, but it is a monolithic structure machined from a single piece of steel. Experimental system dimensions will be given later.

Jointed Beam

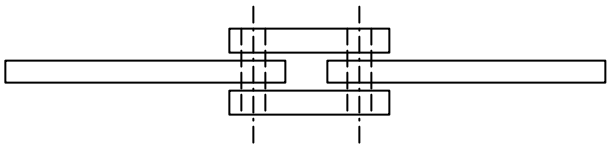

Monolithic Beam

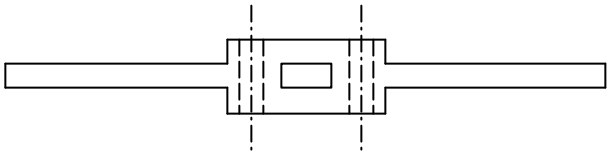

Figure 1. Schematics of Beam Specimens

It is shown later that the two experimental specimens exhibit substantially different dynamic behavior. While their modal frequencies are very close, their damping behaviors are very different. Figure 2 shows why. During vibration the jointed beam system assumes shapes like that shown in Figure 2. At the interface between each beam segment and the plates that support it, longitudinal stress in the beam is great and longitudinal stress in the plates that form the joint is near zero. In view of this slippage (sometimes too small to measure accurately) occurs. Because the surface of any real structure element is rough, to some extent, energy dissipation occurs. It is the effects of this energy dissipation that we seek to characterize trough experiments and to model mathematically.

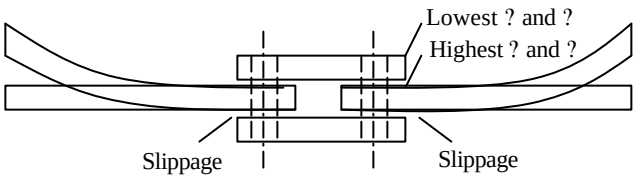

Figure 2. Jointed Beam Schematic.

In the following sections we will (1) describe the experimental configuration and the experiments (2) describe experimental measures of system damping, and show how they can be estimated using measured data, (3) describe an approximate finite element model of the system, and show how it can be used to test friction models for their plausibility, and (4) present numerical and experimental results. Finally, conclusions will be presented and recommendations offered.

2. EXPERIMENTAL CONFIGURATION

The two test structures shown in Figure 1 were evaluated in the experiment. The first structure consisted of two ten inch long steel beams connected by a lap joint. Dimensions are provided in Figure 3. The beam thickness and width are ¼ inch and 1.0 inch respectively. Two ¼ inch steel bolts with washers were used to sandwich the ends of the ten inch beams between two 3 ¼ inch long plates of steel. The bolts were tightened to 85 in-lbs. A ½ inch space was left between the ends of the 10” beams.

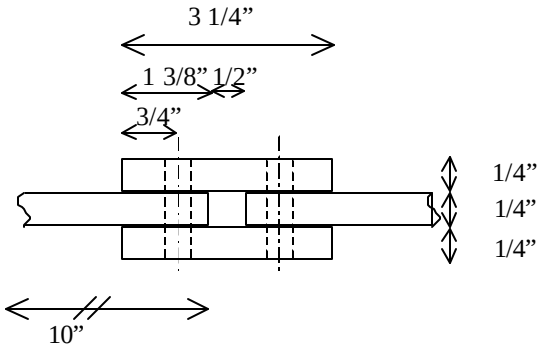

Figure 3. Segmented Beam Geometry

The second structure is an approximate geometric replica of the jointed beam. It is to be used as an experimental control. It was machined from a single piece of steel and shown in Figure 4. Bolts were tightened through the holes in the structure as was done on the jointed beam. This was not required structurally in the solid beam, however, it was done to maintain similarity of the geometry and mass of the two beams.

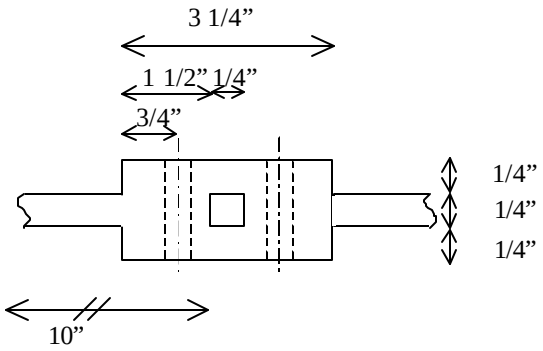

Figure 4. Solid Beam Geometry

During testing the beams were suspended from two approximately 3 ft. long sections of medical tubing in order to simulate a free-free boundary condition. The beams were supported approximately 2 inches from each end. The beams were suspended so that the flexible plane of vibrations was oriented horizontally (Figure 5).

Figure 5. Test Configuration

The beams were instrumented with one Endevco Isotron® 2250A-10 accelerometer fixed with wax to the beam, outside the joint near the center (Figure 6). The accelerometer sensitivity and range were 10.01 mV/g and +/- 500 g respectively. A PCB impact hammer with a white plastic tip was used to excite the beams at various levels. Impacts were applied on the beam center axis, one inch from the end. The force transducer on the hammer (PCB 086C03) has a range of 0-500 lbf. and sensitivity of 10 mV/lbf.

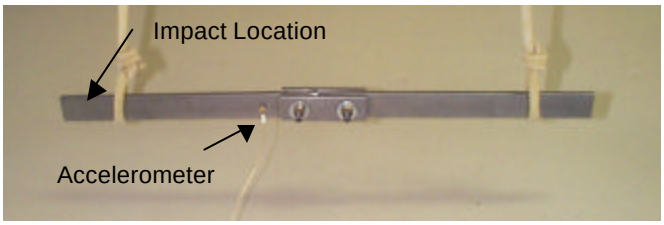

Figure 6. Beam Instrumentation

Force and acceleration data were collected through the Data Physics Corporation ACE DP104 FFT Analyzer two channel data acquisition system using SignalCalc ACE Dynamic Signal Analyzer software on a laptop computer running Microsoft Windows98. Data were recorded for 4.096 s at a rate of 2000 samples/s. This indicates a Nyquist frequency of 1000 Hz. The data were lowpass filtered (for anti-aliasing) at 781 Hz. The AC filter was set to 5 Hz. The data acquisition system was triggered when the hammer force surpassed 5 lbf. A 20 sample buffer was included at the beginning of each run. Twenty runs were averaged to estimate the beam frequency response functions. However, each time response was saved individually. The time histories were exported as ASCII text files to be analyzed in MATLAB. Figure 7 shows estimated frequency response functions for the beams.

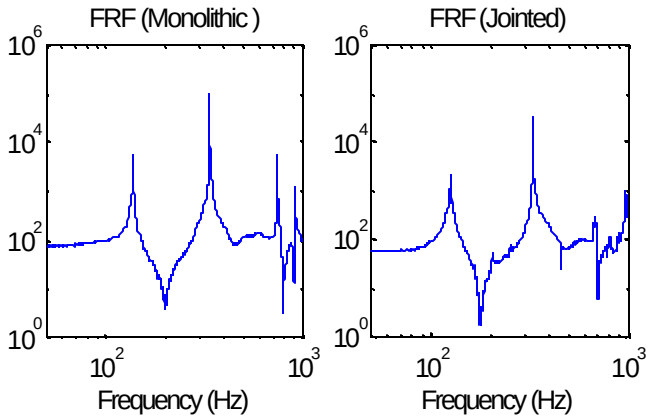

Figure 7. Sample Frequency Response Functions of Jointed and Solid Beams

Though substantial differences in some measures of behavior were anticipated, there are some clearly noticeable similarities. Specifically, the modal frequencies of the two experimental specimens are close. The first three modal frequencies of the jointed beam are 125, 326, and 689 Hz. The first three modal frequencies of the monolithic beam are 137, 339 and 750 Hz. This indicates that the two structures have very similar mass and stiffness characteristics. It is shown later that this similarity does not extend to the dissipative characteristics of the beams.

3. ANALYSIS OF EXPERIMENTAL DATA

Two approaches are used in this investigation to characterize energy dissipation in the beam systems under consideration. First, linear models are used to describe energy dissipation realized in the experimental systems. Later, linear and nonlinear models are used to describe energy dissipation in mathematical models of the physical systems.

Two linear frameworks are used to characterize the beams' experimental behavior realized in the laboratory. These are the log decrement and half power bandwidth frameworks. The log decrement approach is implemented in a local linear construct to approximate energy dissipation in both beams. This is the primary approach to experimental characterization of the beams.

To apply the log decrement approach, the beam was excited as described in the previous section. When the excitation was no longer active, the free decay of the beam was observed. From a separate analysis, the modal frequencies of each beam were assessed. Then each oscillatory decaying acceleration signal was low pass filtered between the first and second oscillatory modes to eliminate higher mode contributions. (Note that two very low frequency rigid body-type modes associated with motion of the beam on its very soft elastic supports did not appear in the data because, as mentioned previously, the measured data were high pass filtered at about 5 Hz.)

To establish the system decay characteristics accurately, the analytic function of the Hilbert transform was computed for each filtered oscillatory signal. This function is an approximate envelope of the signal. In all cases it forms a decaying, approximately exponential curve.

An analysis program divides the decay curve into ten segments that overlap 50 percent. It retains data whose amplitudes are greater than 10 percent of the peak amplitude. The program estimates the average amplitude of the data in each segment. It then takes the natural logarithm of each data segment and fits a straight line to the data using a least squares approach. The system damping factor in the first oscillatory mode is inferred from the parameters of the straight line. The damping factor in each segment is associated with the average amplitude of motion during that segment. Damping versus amplitude is plotted using measurements from several tests. Some results are shown in the experimental results section.

The plots described above supply a visual means for determining system linearity. When the estimates of damping factor plotted as a function of amplitude form a horizontal line, the system mode can be inferred to be linear with damping factor that is constant over all response amplitudes. When the estimates of damping factor plotted as a function of amplitude form a curve with variable ordinate, then the damping coefficient is a nonlinear function of amplitude. When such a curve appears to have a simple form it may be possible to approximate the amplitude dependence of damping factor on displacement or velocity amplitude. The manner in which the damping factors were established implies that these experimental systems can be treated as local linear.

The half power bandwidth estimate uses MATLAB's Transfer Function Estimate (TFE) program to determine the system's frequency response function (FRF). It takes multiple measured acceleration vectors, windows them, and concatenates them to create one continuous vector. Except for windowing, the same is done for the impulsive forces. The excitation and response vectors are inputs to the TFE program. The resulting FRF is input to a modal frequency approximation program, which records the modal frequencies and the corresponding magnitudes of the FRF. The first mode is used for the half power bandwidth analysis. The damping coefficient is estimated in the usual manner. This approach is only used to check the results of the log decrement analysis.

4. MATHEMATICAL MODEL

Simple finite element models of the jointed and monolithic beams were created. The FE models use the structural dynamic framework of the simultaneous ordinary differential equation given by

$$[m]\{\ddot{x}\} + \{R(x, \dot{x})\} = \{q\} \quad (1)$$

where x is displacement at the system degrees of freedom, dot denote differentiation with respect to time, $[m]$ is the mass matrix, $\{R\}$ is the vector of nonlinear restoring force functions (dependent on displacement and velocity), and $\{q\}$ is the forcing function vector. Initial conditions must be specified to solve the equation of motion.

The monolithic beam was modeled in the linear framework. The restoring force governing the system is

$$\{R(x, \dot{x})\} = [c]\{\dot{x}\} + [k]\{x\} \quad (2)$$

where $[c]$ and $[k]$ are the viscous damping and stiffness matrices.

The operations of the FE code include (among other things) synthesis of the mass and stiffness matrices, eigenvalue analysis (for linear problems), and solution of the system of ordinary differential equations. The code is implemented in MATLAB. Beam elements with two degrees of freedom (rotational and translational) are used to construct the stiffness and mass matrices. The mass matrix is diagonal. The built in eigenvalue analysis (eig) is

used to solve the eigenvalue problem. The results are presented later.

Jointed beam analysis requires the capability to solve nonlinear ordinary differential equations. The nonlinear behavior is approximated by simplifying equation 1 by constraining system motion to a single linear mode. Specifically, the vector displacement and velocity responses of the system were approximated using

$$\{x(t)\} = \sum_k \phi_k(t)\{\psi_k\}, \{\dot{x}(t)\} = \sum_k \dot{\phi}_k(t)\{\psi_k\} \quad (3)$$

where $\phi_k(t)$ is displacement in the kth modal coordinate, $\dot{\phi}_k(t)$ is the corresponding velocity and ψ_k is the kth orthanormal mode shape. It is recognized that this approximation can never converge to the exact solution. However, experimental observations indicate that this is an accurate approximation. Thus the restoring force for the nonlinear system is modeled as

$$\{R(x,\dot{x})\} = [c]\{\dot{x}\} + [k]\{x\} + \{R_{nl}(x,\dot{x})\} \quad (4)$$

General system damping is modeled as viscous. $\{R_{nl}(x,\dot{x})\}$ is zero except where degrees of freedom are attached with nonlinear elements.

Figure 7 shows a schematic of part of the FE model. Beam elements are shown as blocks. The nonlinear connections are included in $\{R_{nl}(x,\dot{x})\}$.

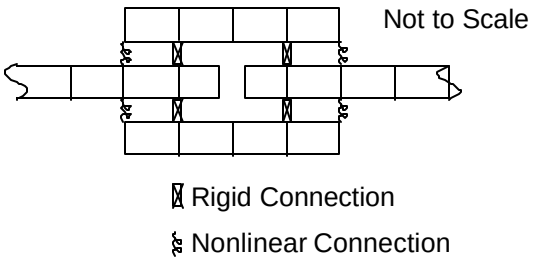

Figure 7. Nonlinear Finite Element Model Schematic

Friction is modeled using a form of the bristles construct often referred to as the Lu-Gre model (see Gaul and Nitche and Haessing and Friedland, 1991). The assumptions underlying the model follow. Opposing frictional surfaces are irregular and the irregularities can be modeled with bristles. When opposing surfaces move relative to one another some bristles establish and/or maintain contact while others lose contact. The bristles in contact and this results in a displacement related motion resistance. Based on experimental evidence, it is assumed that the fraction of bristles in contact is a function of velocity. Based on these assumptions the restoring force, opposing motion at the frictional joint is

$$R = \mu N k |\Delta x| \quad (4)$$

where μ = average fraction of bristles in contact, N = number of bristles, k = bristle stiffness, Δx = change in displacement over time interval of interest. For this investigation μ was given the form

$$\mu = \mu_0 e^{-v^2/2\sigma^2} + \mu_1 \quad (5)$$

where σ, μ_0, and μ_1 are parameters of the model. A typical example of μ is shown in Figure 8.

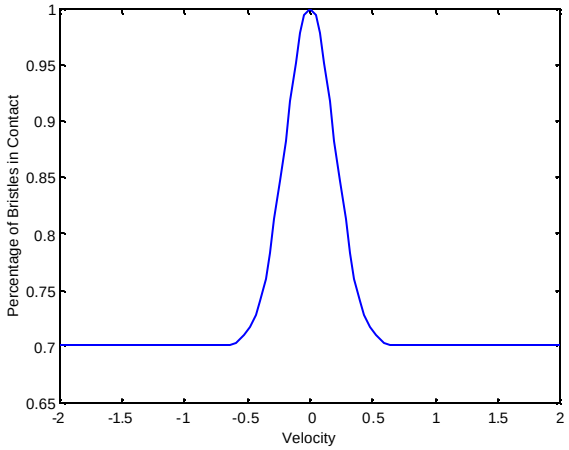

Figure 8. Percentage of bristles in contact, $\mu(v)$

Our experimental results (summarized in the following section) showed that the bristle model incorrectly predicts the qualitative behavior of the lap jointed beam. The model can be modified by inserting explicit dependence on velocity. When this is done, energy dissipation in the mathematical model of the beam can be made to match the experimental results. The model we chose to use is

$$R = v^{\frac{1}{4}} \mu N k |\Delta x| \quad (6)$$

This restoring force equals zero at zero velocity. A graph showing the relationship of the restoring force to velocity and change in displacement, $R(v,\Delta x)$, is shown in Figure 9.

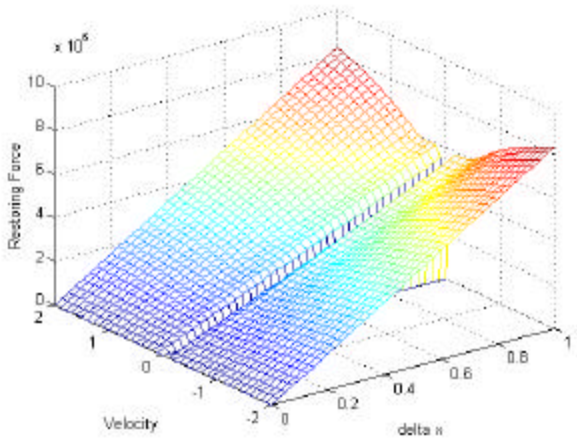

Figure 9. Absolute value of restoring force, $R(v,\Delta x)$

5. EXPERIMENTAL RESULTS

The experiments described in a previous section were performed and system excitations and responses were measured. Two measured acceleration response time histories are shown in Figures 10 and 11. The first is the low pass filtered acceleration response of the jointed beam with filter cutoff frequency of 240 Hz. The second is the low pass filtered acceleration response of the monolithic beam with filter cutoff frequency of 240 Hz. Below each time history is the envelope formed by the analytic function of the Hilbert transform of the response time history. Though not apparent from the time histories, the fundamental frequency of response of the jointed beam is 125 Hz, and that of the monolithic beam is 137 Hz. It is clear from the graphs that the average decay rates of the jointed and monolithic beams differ greatly.

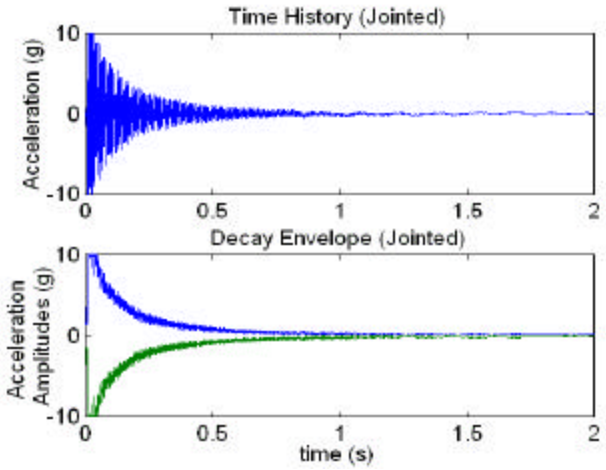

Figure 10. Typical response time history and its envelope for the jointed beam.

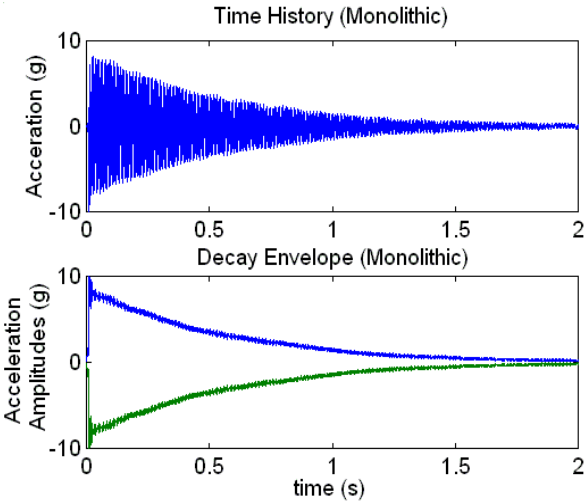

Figure 11. Typical response time history and its envelope for the monolithic beam.

The amplitude decay signals were analyzed as specified in the Analysis of Experimental Data Section. Local linear estimates of damping factors were computed for both beams and are shown in Figures 12 and 13. Both figures depict local linear estimates of damping factors as a function of velocity amplitude. The former presents this information for the monolithic beam; the latter for the jointed beam. Each figure presents the results of 20 tests. The data are scattered because (1) the measurements include random noise, and (2) the system, environment, and boundary conditions vary slightly from one test to the next.

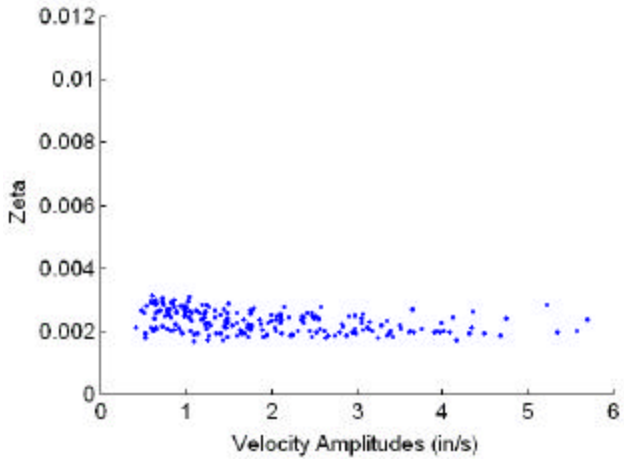

Figure 12. Estimates of local linear damping factor versus velocity amplitude for the monolithic beam.

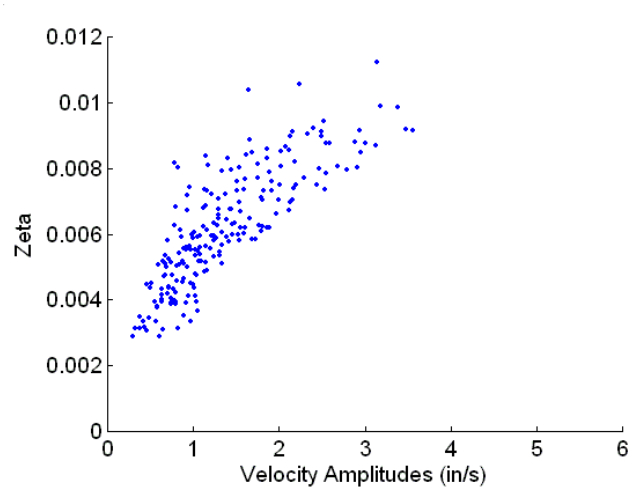

Figure 13. Estimates of local linear damping factor versus velocity amplitude for the jointed beam.

The data in Figure 12 appear to indicate that damping level is constant with respect to amplitude, for the monolithic beam, over the range of amplitudes considered in these experiments. The sample mean of the damping factor estimates in Figure 12 is 0.22 percent.

In contrast, the data in Figure 13 show that damping increases with velocity amplitude in the jointed beam. Over the range of amplitudes considered in those experiments local linear damping factor estimates vary from about 0.3 percent at an amplitude of 0.5 in/s to about one percent at an amplitude of 3.5 in/s. It is clear that the slope of the mean of the damping factors diminishes with increasing velocity amplitude. This is to be expected because (1) damping effects cannot increase without bound, and (2) the physical phenomenon may restrict damping effects to some upper limit.

The average damping factor of the two systems was estimated using the half power bandwidth approach. The damping factor of the monolithic beam was estimated to be 0.24 percent, and that of the jointed beam was estimated to be 0.64 percent. These values tend to confirm the results shown in Figures 12 and 13, because they represent averages formed using responses at all levels.

6. ANALYTICAL RESULTS

The linear and nonlinear analyses described in the Mathematical Model Section were performed with the objective of simulating the behavior of the two experimental systems. Both linear and nonlinear analyses are modal-based. The response in a single mode is considered. This modal analysis is exact for the linear system, but only an approximation for the nonlinear system.

Modal frequencies for the linear system were estimated as 134, 333, and 730 Hz (versus 137, 339, and 750 Hz, for the monolithic experimental system). The modal analysis that forms the basis for analysis of the nonlinear beam yielded modal frequencies of 116, 339, and 624 Hz (versus 125, 326, and 689 for the jointed experimental system). The reason for the differences between the analyzed modal frequencies and those experimentally obtained is primarily the imperfection of the mathematical models. The form of the friction model is given in Eq. (5). The parameters used in this investigation are: ?? = 0.2, ? = 0.3, $?_1$ = 0.7 and Nk = 2.5 x 10^9.

The analyzed velocity response time histories of the linear and nonlinear beams in their first oscillatory modes are shown in Figures 14 and 15, along with their envelopes as represented by the analytic function of the Hilbert transform. (Velocity is shown because only displacement and velocity are computed.)

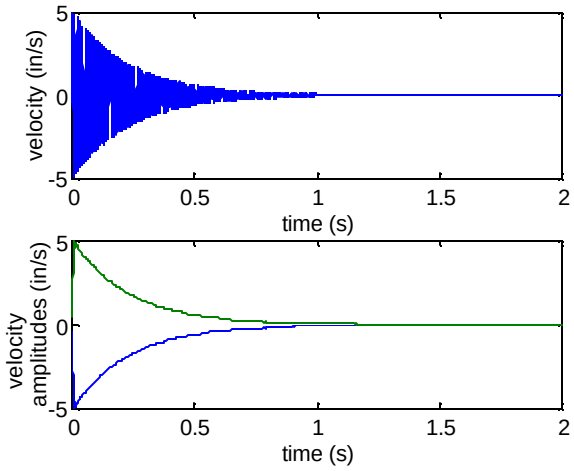

Figure 14. Computed velocity response of linear system, and its envelope.

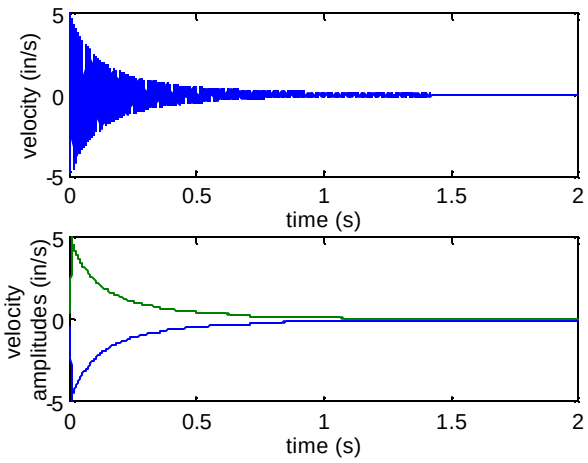

Figure 15. Computed velocity response of nonlinear system, and its envelope.

The analyzed time histories clearly mimic the experimental measurements. That is, the simulated motion in the jointed beam decays more rapidly than the corresponding motion in the monolithic beam. Further, the frequencies of motion accurately duplicate the fundamental frequencies of the experimental beams, but this should be expected because the modal approximation forces motion to occur at a particular frequency.

As for the experimental data, local linear damping factor estimates from the analyzed responses were computed. The results are shown in Figures 16 and 17.

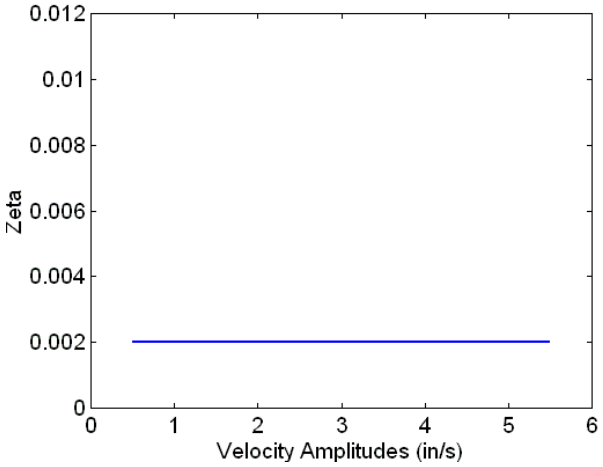

Figure 16. Estimates of local linear damping factor versus velocity amplitude for the linear beam model.

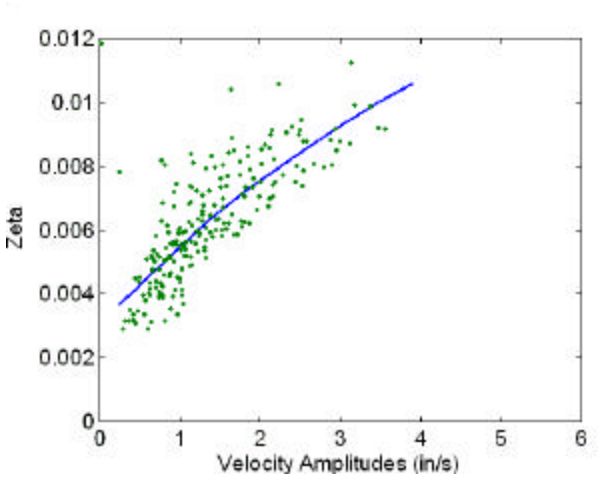

Figure 17. Estimates of local linear damping factor versus velocity amplitude for the nonlinear beam model (solid line). The data from Figure 13 are also shown for reference.

Figure 16 shows that damping in the linear model is a constant. This is appropriate because it is constrained to be so.

Figure 17 shows that the local linear damping factor in the nonlinear beam model is variable and resembles the mean of the experimental data obtained from experiments on the jointed beam. This shows that the mathematical model for friction given by Eq. (6) plausibly explains energy dissipation in the jointed beam. Though Figure 17 demonstrates the plausibility of the modified bristle model, much more experimentation and analysis are required to demonstrate its optimality.

7. CONCLUSIONS

Experiments were performed on two simple geometrically identical beams to characterize nonlinear lap joint behavior. The beams were impact tested and response decay characteristics were used to infer modal damping. The experimental results were cast as local linear damping factor versus velocity amplitude. A monolithic beam displayed constant damping behavior. A lap jointed beam displayed damping that is an increasing function of amplitude.

Approximate analyses were performed to test the plausibility of a model for joint friction. Both linear and approximate nonlinear finite element models for beam behavior were developed. The modal frequencies of the linear model matched the corresponding values for the monolithic system closely. The approximate nonlinear analysis was used to develop the relation between local linear damping factor and velocity amplitude. The analytical results matched the experimental results closely. This demonstrates the plausibility of the bristle model.

Though the bristle construct appears to offer a plausible, phenomenological alternative for modeling joint friction, the authors recommend that further study be conducted prior to adoption in specific applications. Physical systems and their mathematical models should be exercised and validated using other methods and forms of excitation.

Finally, to establish a useful mathematical model for friction, predictive rules for designing and analyzing joints in complex systems are required.

ACKNOWLEDGEMENTS

The authors wish to acknowledge the Department of Energy and Los Alamos National Laboratory for their support of the Los Alamos Dynamics Summer School.

REFERENCES

Gaul L., Nitsche R. “The Role of Friction in Mechanical Joints,” Submitted for publication.

Haessing D. A., Jr., Friedland B. (1991), “On the Modeling and Simulation of Friction,” *Journal of Dynamics Systems , Measurements, and Control.*

Haug Edward J. (1992) *Intermediate Dynamics*, Prentice Hall, Eaglewood Cliffs, New Jersey.

Inman D. J. (1996), *Engineering Vibration*, Prentice Hall, Upper Saddle River.

Ottl D., (1981), “Schwingungeng mechanischer systeme mit Strukturdampfung,” Number 603. VDI-Fortschritt-Berichte, Dusseldorf.

Stribeck R. (1902) “Die wesentlichen Eigenschaften der Gleitund Rollenlager - The key qualities of sliding and roller bearings,” Zeitschrift des Vereins deutsher Ingenieure, 46(38,39):1342-48.1432-37.